

Next-to-next-to-leading order event generation for Z-boson production in association with a bottom-quark pair

Javier Mazzitelli¹, Vasily Sotnikov², Marius Wiesemann³

¹ *Paul Scherrer Institut, CH-5232 Villigen PSI, Switzerland*

² *Physik Institut, Universität Zürich, CH-8057 Zürich, Switzerland and*

³ *Max-Planck-Institut für Physik, Boltzmannstraße 8, 85748 Garching, Germany*

We consider the production of a Z boson decaying to leptons in association with a bottom-quark pair in hadronic collisions. For the first time, we compute predictions at next-to-next-to-leading order (NNLO) in QCD, and we combine them with the all-orders radiative corrections from a parton-shower simulation (NNLO+PS). Our method represents the first approach to NNLO+PS event generation applicable to processes featuring a colour singlet and a heavy-quark pair in the final state. The novel two-loop corrections are computed for massless bottom quarks, and the leading mass corrections are restored through a small-mass expansion. The calculation is carried out in the four-flavour scheme, and we find that the sizeable NNLO QCD corrections lift the long-standing tension between lower-order predictions in four- and five-flavour schemes. Our predictions are compared to a CMS measurement for Z boson plus b -jet production, achieving an excellent description of the data.

Introduction.—The quest to uncover signals of new physics at the Large Hadron Collider (LHC) has become a major endeavour within the extensive physics program of the LHC experiments, encompassing both the direct detection of resonances and the analysis of small deviations from the Standard Model (SM) through precision measurements. The success of the latter critically depends on the availability of highly accurate simulations and predictions for all classes of LHC reactions.

The associated production of a Z boson and a bottom-quark pair ($b\bar{b}Z$) plays a special role in the LHC physics program. For one, it yields heavy-quark mass effects to Drell-Yan production, a process that is measured very accurately at hadron colliders and used to extract the mass of the W boson, see e.g. Refs. [1–3]. Moreover, $b\bar{b}Z$ production is a major background to ZH measurements [4, 5] and to various BSM searches, see e.g. Ref. [6].

Precision measurements of Z -boson production with bottom-flavoured jets (b -jets) have been performed both at the Tevatron [7–9] and by the LHC experiments [10–17]. So far, there has been a significant discrepancy among the $Z+b$ -jet theory predictions, depending on whether the bottom quark is assumed to be massive in a four-flavour scheme (4FS) or massless in a five-flavour scheme (5FS) calculation [18]. Especially, state-of-the-art 4FS predictions are in tension with measurements of $Z+b$ -jet production [10, 11, 13, 14, 18].

Next-to-leading-order (NLO) corrections in QCD have been computed both in the 4FS [19] (see also Ref. [20]) and in the 5FS [21]. In the 5FS, Z boson production with a single b -jet is known through next-to-next-to-leading-order (NNLO) [22]. Refs. [19, 23] showed that the inclusion of bottom-mass effects in the 4FS is important for the $b\bar{b}Z$ cross section and in kinematic distributions of the bottom quarks for scales close to m_b . The matching of the NLO corrections with a parton shower (NLO+PS) is available in both schemes within MADGRAPH5_AMC@NLO [24] and within SHERPA [18],

where the 5FS implementation in SHERPA includes up to two extra b -jets at NLO+PS via multi-jet merging. The combination of four- and five-flavour predictions at NLO+PS was achieved in Ref. [25], see also Ref. [26] for an earlier study. Higher-order corrections to $b\bar{b}Z$ production are substantial, especially in the 4FS, with very sizeable perturbative uncertainties. Prior to this work, no NNLO results had been obtained for any of the flavour schemes.

In this letter we considerably improve the accuracy of $Z+b$ -jet theory predictions by computing the NNLO QCD corrections to $b\bar{b}Z$ production for massive bottom quarks. Our results are implemented in a fully exclusive Monte Carlo event generator by matching the NNLO corrections to a parton shower (NNLO+PS). Our approach represents the first NNLO+PS method for such an involved final state, featuring both a heavy-quark pair and a set of colour-singlet particles. The two-loop corrections for the $b\bar{b}Z$ process are presented here for the first time, by exploiting the massless amplitudes [27] to approximate the massive ones. We use our novel results to investigate whether the NNLO corrections resolve the long-standing discrepancies between 4FS and 5FS predictions, and compare our results with the latest $Z+b$ -jet measurement by CMS [15] to assess their impact on the tension of previous 4FS predictions with LHC data.

Methodology.—We consider the process

$$pp \rightarrow b\bar{b}\ell^+\ell^- + X, \quad (1)$$

which we denote as $b\bar{b}Z$ production for brevity. Sample Feynman diagrams at the leading order (LO) are shown in Figure 1. They involve both quark- and gluon-initiated channels, where the Z boson can be radiated off any of the quark lines.

Among the NNLO+PS frameworks for colour-singlet production [28–32], only the MINNLO_{PS} approach [31],

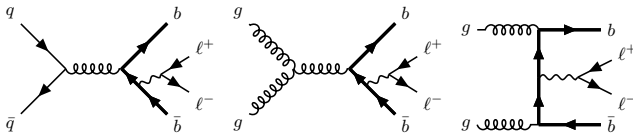


FIG. 1. Feynman diagrams for $pp \rightarrow b\bar{b}l^+l^-$ at LO.

[32] has been extended to processes featuring colour charges in initial and final state, namely heavy-quark pair production [33–35]. We further extend the MINNLO_{PS} method to construct a fully exclusive NNLO+PS generator for the associated production of a heavy quark pair ($Q\bar{Q}$) with a system colour-singlet particles (F).

The general structure of large logarithmic contributions at small transverse momentum for $Q\bar{Q}$ and $Q\bar{Q}F$ production is very similar [36]. As a result, we can exploit the analytic formula for the cross section differential in the transverse momentum $p_T \equiv |\vec{p}_T|$ and the Born phase space Φ_B of the final-state system, which was derived in Refs. [33, 34] from the well-known factorization theorem for $Q\bar{Q}$ production at small p_T [37–40] and reads

$$\frac{d\sigma}{dp_T d\Phi_B} = \frac{d}{dp_T} \left\{ \sum_c \left[\sum_{i=1}^{n_c} \mathcal{C}_{c\bar{c}}^{[\gamma_i]} e^{-\tilde{S}_{c\bar{c}}^{[\gamma_i]}} \right] \mathcal{L}_{c\bar{c}} \right\} + R_f. \quad (2)$$

The first term includes the singular (and constant) contributions in p_T , which represents the transverse momentum of the $Q\bar{Q}F$ system here, while R_f adds the regular contributions.

This formula retains NNLO plus LL accuracy, and it preserves the class of NLL corrections that traditional PS algorithms [41] include. Therefore, it is the starting point to build a Monte Carlo algorithm for the generation of NNLO events within the POWHEG framework [42, 43], which has been demonstrated several times [31, 32, 34], most recently for $Q\bar{Q}$ production in Ref. [34]. In the following, instead, we focus on the main changes from $Q\bar{Q}$ to $Q\bar{Q}F$ processes.

The sum over c in Eq. (2) runs over the flavour configurations $\{g, q, \bar{q}\}$ of the incoming partons of flavour c and \bar{c} , while the sum over i originates from diagonalizing the one-loop soft anomalous dimension $\mathbf{\Gamma}^{(1)}$ with complex coefficients $\mathcal{C}_{c\bar{c}}^{[\gamma_i]}$, where n_c is determined by the SU(3) representation of a given flavour configuration.¹ The eigenvalues of $\mathbf{\Gamma}^{(1)}$, denoted by γ_i , induce a modification to the Sudakov exponent, as indicated by the notation $\tilde{S}_{c\bar{c}}^{[\gamma_i]}$. We note that $\mathbf{\Gamma}^{(1)}$, its eigenvalues, and the coefficients stemming from its diagonalization have the same form as for $Q\bar{Q}$ production (see Appendix A of Ref. [34]) after adapting the process-dependent LO matrix $\mathbf{H}^{c\bar{c}}$, which enters the definition of $\mathcal{C}_{c\bar{c}}^{[\gamma_i]}$. We construct this matrix

from colour-decomposed scattering amplitudes of OPENLOOPS [44–46]. Contributions from $\mathbf{\Gamma}^{(2)}$ are included in the Sudakov with an approximation of its corrections beyond NNLO. The general form of $\mathbf{\Gamma}^{(2)}$ includes terms proportional to three parton correlations, whose expectation value with the LO matrix element vanishes in the $Q\bar{Q}$ case. For $Q\bar{Q}F$ processes they contribute, and we therefore include them in our implementation.

The last ingredient of Eq. (2) is the luminosity factor

$$\mathcal{L}_{c\bar{c}} \equiv \frac{|M_{c\bar{c}}^{(0)}|^2}{2m_{Q\bar{Q}F}^2} \sum_{i,j} \left[\text{Tr}(\tilde{\mathbf{H}}_{c\bar{c}} \mathbf{D})(\tilde{C}_{ci} \otimes f_i)(\tilde{C}_{\bar{c}j} \otimes f_j) \right]_{\phi} \quad (3)$$

with the LO matrix element $M_{c\bar{c}}^{(0)}$, the invariant mass of the $Q\bar{Q}F$ system $m_{Q\bar{Q}F}$, and the convolution, denoted by the operation \otimes , of the collinear coefficient functions \tilde{C}_{ij} with the parton densities f_i . Quantities in bold face are operators in colour space, and the trace $\text{Tr}(\tilde{\mathbf{H}}_{c\bar{c}} \mathbf{D})$ runs over the colour indices. The symbol $[\dots]_{\phi}$ denotes the average over the azimuthal angle ϕ of \vec{p}_T , and the operator of azimuthal correlations \mathbf{D} is defined such that $[\mathbf{D}]_{\phi} = 1$.

The notation $\text{Tr}(\tilde{\mathbf{H}}_{c\bar{c}} \mathbf{D})(\tilde{C}_{ci} \otimes f_i)(\tilde{C}_{\bar{c}j} \otimes f_j)$ is symbolic. In particular, the gluon-initiated channel features a richer Lorentz structure, typically denoted by additional G functions [47], which encode azimuthal correlations of collinear origin and are kept implicit here. Therefore, the product of $\text{Tr}(\tilde{\mathbf{H}}_{c\bar{c}} \mathbf{D})$ and $(\tilde{C}_{ci} \otimes f_i)(\tilde{C}_{\bar{c}j} \otimes f_j)$ should be understood as a tensor contraction, which leads to additional azimuthal correlations, see Ref. [39]. These contributions enter our calculation as terms proportional to $\langle M_{gg}^{(0)} | \mathbf{D}^{(1)} | M_{gg}^{(0)} \rangle \times G^{(1)}$. They were computed analytically for $Q\bar{Q}$ production in Ref. [48]. For $Q\bar{Q}F$ processes we compute them through a numerical integration over the azimuthal angle in conjugate space (b space). Similarly, we adapt the implementation of the $G^{(1)} \times G^{(1)}$ contribution, which we extract using OPENLOOPS.

After accounting for the azimuthal correlations in the trace with the hard-virtual operator $\tilde{\mathbf{H}}_{c\bar{c}}$ in Eq. (3), we evaluate its contribution as

$$H_{c\bar{c}} = \frac{\langle \mathcal{R}_{c\bar{c}} | \bar{\mathbf{h}}^\dagger \bar{\mathbf{h}} | \mathcal{R}_{c\bar{c}} \rangle}{\langle \mathcal{R}_{c\bar{c}}^{(0)} | \mathcal{R}_{c\bar{c}}^{(0)} \rangle}, \quad \bar{\mathbf{h}} | \mathcal{R}_{c\bar{c}} \rangle = \bar{\mathbf{h}} \mathbf{Z}^{-1} | \mathcal{M}_{c\bar{c}} \rangle, \quad (4)$$

where $\mathcal{R}_{c\bar{c}}$ is the finite remainder obtained from the virtual amplitude $\mathcal{M}_{c\bar{c}}$ after removing the IR divergences through the operator \mathbf{Z}^{-1} [49, 50], $\langle \mathcal{R}_{c\bar{c}}^{(0)} | \mathcal{R}_{c\bar{c}}^{(0)} \rangle = |M_{c\bar{c}}^{(0)}|^2$, and the operator $\bar{\mathbf{h}}$ determines parton emissions of soft origin, which are known for $Q\bar{Q}$ production up to NNLO [51]. Here, we employ their extension to the general kinematics of $Q\bar{Q}F$ production [52].

The process-dependent pieces entering the hard function are the finite remainders up to two loops. We obtain the one-loop amplitude entering $H_{c\bar{c}}^{(1)}$ and one-loop squared amplitude entering $H_{c\bar{c}}^{(2)}$ from OPENLOOPS. While all other contributions are taken exactly, we calculate the two-loop finite remainder $2 \text{Re} \langle \mathcal{R}_{c\bar{c}}^{(0)} | \mathcal{R}_{c\bar{c}}^{(2)} \rangle$ entering $H_{c\bar{c}}^{(2)}$ in an approximation, since its full computation

¹ The notation $X^{(i)}$ denotes the i -th term in the perturbative expansion of the quantity X with respect to $\alpha_s/(2\pi)$.

is well beyond current technology for two-loop 5-point amplitudes. Realizing that there is a hierarchy in the bottom-quark mass m_b , we can perform an expansion around small m_b of the two-loop amplitude, capturing the constant and logarithmically enhanced terms in m_b , while omitting power corrections in m_b :

$$\frac{2 \operatorname{Re} \langle \mathcal{R}_{c\bar{c}}^{(0)} | \mathcal{R}_{c\bar{c}}^{(2)} \rangle}{\langle \mathcal{R}_{c\bar{c}}^{(0)} | \mathcal{R}_{c\bar{c}}^{(0)} \rangle} = \frac{2 \operatorname{Re} \langle \mathcal{R}_{0,c\bar{c}}^{(0)} | \mathcal{R}_{0,c\bar{c}}^{(2)} \rangle}{\langle \mathcal{R}_{0,c\bar{c}}^{(0)} | \mathcal{R}_{0,c\bar{c}}^{(0)} \rangle} + \sum_{i=0}^4 \kappa_{c\bar{c},i} \log \left(\frac{m_b}{\mu_R} \right)^i + \mathcal{O} \left(\frac{m_b}{\mu_h} \right), \quad (5)$$

where $\mathcal{R}_{0,c\bar{c}}^{(i)}$ denotes the finite remainder of the *massless* $b\bar{b}Z$ amplitude, i.e. setting $m_b = 0$, μ_R is the renormalization scale, and μ_h is a characteristic hard scale of the process. The process-dependent coefficients $\kappa_{c\bar{c},i}$ are determined in Appendix A. They are obtained through a *massification* procedure that relates the $1/\epsilon^i$ poles of collinear origin in the 5FS with logarithmic terms in m_b in the 4FS [53, 54], see also Ref. [55] for a recent application to $b\bar{b}W$ production.

In the massless case, the calculation of the two-loop amplitude is still very challenging, but feasible [27]. While the logarithmic terms are reproduced without any approximations, $\operatorname{Re} \langle \mathcal{R}_{0,c\bar{c}}^{(0)} | \mathcal{R}_{0,c\bar{c}}^{(2)} \rangle$ is computed in the leading-colour approximation (LCA), with the exception of contributions of Z/γ^* bosons coupling to closed fermion loops, which are omitted. We have tested the latter to be negligible already at the one-loop level (see also Refs. [56, 57]). The LCA is typically accurate within 10% (see e.g. Refs. [58, 59]). Since the numerical effect of $\langle \mathcal{R}_{0,c\bar{c}}^{(0)} | \mathcal{R}_{0,c\bar{c}}^{(2)} \rangle$ on the MINNLO_{PS} cross section is typically at the few-percent level, we expect these approximations to have a negligible impact on our results. To calculate $\operatorname{Re} \langle \mathcal{R}_{0,c\bar{c}}^{(0)} | \mathcal{R}_{0,c\bar{c}}^{(2)} \rangle$ we have implemented a numerical code based on the analytic results of Ref. [27], employing the PENTAGONFUNCTIONS++ code [60–62] to evaluate the relevant special functions.

We note that our calculation of the logarithmically enhanced terms in Eq. (5) has been rendered possible for closed massive fermion loops only by the recent results of Ref. [54]. The numerical impact of those contributions is at the few-percent level of the NNLO cross section.

Since our NNLO+PS generator assumes massive bottom quarks, a mapping from the massive to the massless phase space is required to evaluate the massless remainders $\mathcal{R}_{0,c\bar{c}}^{(i)}$. While different mappings induce only power corrections in m_b/μ_h , it is mandatory that the mapping avoids the collinear singularities of the massless amplitudes, which in the massive phase space are prevented by the bottom mass.² We have tested different map-

pings and found their results to agree at the sub-percent level. The details are given in Appendix B.

Results.—For the phenomenological study of $b\bar{b}Z$ production at NNLO+PS we focus on LHC collisions with 13 TeV centre-of-mass energy and consider the leptonic final states with $\ell = e, \mu$. The bottom and top-quark on-shell masses are set to 4.92 GeV and 173.2 GeV, respectively, with four massless quark flavours. We employ the corresponding NNLO set of the NNPDF31 [63] parton densities with $\alpha_s(m_Z) = 0.118$. We use the complex-mass scheme [64, 65] and the electroweak (EW) input parameters are set in the G_μ scheme using [66]: $G_F = 1.16639 \times 10^{-5} \text{ GeV}^{-2}$, $M_W = 80.385 \text{ GeV}$, $\Gamma_W = 2.0854 \text{ GeV}$, $m_Z = 91.1876 \text{ GeV}$, $\Gamma_Z = 2.4952 \text{ GeV}$. Unless specified otherwise, our default choice for the renormalization scale of the two powers of the α_s at Born-level is $\mu_R^{(0)} = m_{b\bar{b}\ell\ell}$. The scale of extra powers of α_s in the radiative corrections and the factorization scale are set following the MINNLO_{PS} prescription [31, 34]. We employ the definition of the modified logarithm L in Ref. [34], which smoothly turns off resummation effects for p_T values larger than $Q = m_{b\bar{b}\ell\ell}/2$. To avoid the Landau singularity at small p_T , the scale of the strong coupling and the parton densities is smoothly frozen around $Q_0 = 2 \text{ GeV}$ [32]. Scale uncertainties are estimated through the usual 7-point scale variations by a factor of two around the central scale. As a parton shower we employ PYTHIA8 [67] with the Monash tune [68].

For comparison, we implemented a generator for $pp \rightarrow b\bar{b}\ell^+\ell^-$ production at NLO+PS in the 4FS within POWHEG-BOX-RES [43]. In this case we use $m_{b\bar{b}\ell\ell}$ for the central scales. We also evaluate MINLO' results, which are NLO accurate for $b\bar{b}\ell^+\ell^-$ plus zero and one jet, by turning off the NNLO corrections in the MINNLO_{PS} generator.

Table I shows the $pp \rightarrow b\bar{b}\ell^+\ell^-$ total cross section. For reference, NLO+PS (MINNLO_{PS}) results with a central scale $H_T/2$ ($\mu_R^{(0)} = H_T/2$) are given as well, where H_T is the sum over the transverse masses of each bottom quark and each lepton. Shower effects are negligible for the inclusive rate and we keep effects from hadronization,

	σ_{total} [pb]	ratio to NLO
NLO+PS ($m_{b\bar{b}\ell\ell}$)	32.21(0) ^{+16.4%} _{-13.4%}	1.000
MINLO' ($m_{b\bar{b}\ell\ell}$)	22.33(1) ^{+28.2%} _{-17.9%}	0.693
MINNLO _{PS} ($m_{b\bar{b}\ell\ell}$)	51.23(4) ^{+17.3%} _{-12.4%}	1.591
NLO+PS ($H_T/2$)	40.14(1) ^{+18.9%} _{-15.0%}	1.000
MINNLO _{PS} ($H_T/2$)	58.70(4) ^{+19.0%} _{-13.1%}	1.462

TABLE I. Total $b\bar{b}Z$ cross section with $66 \text{ GeV} \leq m_{\ell^+\ell^-} \leq 116 \text{ GeV}$. The scale in brackets indicates the different scale setting as described in the text. The quoted errors represent scale uncertainties, while the numbers in brackets are numerical uncertainties on the last digit.

² We thank Chiara Savoini and Massimiliano Grazzini for bringing this to our attention.

multi-parton interactions (MPI) and QED radiation off.

The MINLO' prediction, which is formally NLO accurate and includes additional $\mathcal{O}(\alpha_s^2)$ corrections, is 44% smaller than the other NLO+PS result and does not provide a reasonable prediction. Although this may seem surprising, this behaviour can be explained by the substantial cancellation of logarithmic corrections in m_b between the real (double-real and real-virtual) and the double-virtual amplitudes. Those logarithmic terms originate from the massive bottom quark in the 4FS, which regulates the real phase-space integration as well as the loop integration. The ensuing logarithmic contributions are bound to cancel between real and double-virtual amplitudes, which can be understood by considering the 5FS, where these logarithms would appear as $1/\epsilon$ poles that cancel by the KLN theorem [69, 70].

For MINLO', the relative $\mathcal{O}(\alpha_s^2)$ contribution is incomplete as only the real amplitudes are included and the corresponding logarithmic terms induce a numerically significant negative effect. We have checked that it is sufficient to include the logarithmic corrections in the double-virtual amplitudes (obtained using the massification procedure in Appendix A) to restore the appropriate cancellation and obtain a positive $\mathcal{O}(\alpha_s^2)$ correction. Due to this unphysical effect we refrain from including MINLO' results in the remainder of this letter.

Considering the MINNLO_{PS} predictions in Table I, NNLO corrections increase the NLO cross section by almost 60%, which renders them crucial for an accurate prediction in the 4FS. Since the NNLO corrections are much larger than the NLO scale uncertainties, we consider $H_T/2$ as a second scale choice. In this case, the NLO and the NNLO cross sections are larger, with NNLO corrections of about 46%. It is reassuring that the dependence on the scale choice reduces at NNLO compared to NLO.

In Table II we consider the fiducial cross section measurement of the most recent CMS analysis for Z -boson production in association with bottom-flavoured jets (b -jets) [15], which includes the complete Run-2 data set of the LHC. The fiducial cuts are defined in Appendix C. To warrant a realistic comparison to data we include effects from hadronization, multi-parton interactions (MPI) and QED radiation from now on. In our 4FS calculation, we

σ_{fiducial} [pb]	$Z+\geq 1$ b -jet	$Z+\geq 2$ b -jets
NLO+PS (5FS) [15]	7.03 ± 0.47	0.77 ± 0.07
NLO+PS (4FS)	4.08 ± 0.66	0.44 ± 0.08
MINNLO _{PS} (4FS)	6.85 ± 0.98	0.80 ± 0.11
CMS [15]	6.52 ± 0.43	0.65 ± 0.08

TABLE II. Comparison of theory predictions with the fiducial cross-section measurements by CMS [15] for (at least) one and two tagged b -jets. Experimental uncertainties are added in quadrature. The 5FS result is taken from Ref. [15] and scale uncertainties have been symmetrized by taking the maximum of the absolute value of the errors.

can directly apply the experimental definition of b -jets, which is rendered infrared safe by the bottom mass, while in the 5FS the naive definition of b -jets leads to divergences [71–75]. For the $Z+\geq 1(2)$ b -jet rate we observe a clear tension with the NLO+PS result in the 4FS, whose central cross section is 40(20)% below the measurement, well outside the uncertainties. By contrast, the MINNLO_{PS} prediction is in full agreement with the data within uncertainties.

In addition, we include in Table II the NLO+PS prediction in the 5FS, as quoted in the CMS analysis [15] and obtained with MADGRAPH5_AMC@NLO [76].³ NLO+PS results in 4FS and 5FS are not compatible with each other, but our MINNLO_{PS} prediction agrees with the 5FS result, thanks to the inclusion of NNLO QCD corrections in the 4FS. While both predictions agree similarly well with the $Z+\geq 2$ b -jets data, MINNLO_{PS} shows a slightly better description in the $Z+\geq 1$ b -jet fiducial region.

Next, we examine a set of differential distributions in Fig. 2 and compare NLO+PS (blue, dashed) and MINNLO_{PS} (red, solid) predictions to the CMS measurement (black data points) [15]. The first three figures show observables in the inclusive 1- b -jet phase space: the transverse momentum ($p_T^{b\text{-jet}1}$) and pseudo-rapidity ($\eta^{b\text{-jet}1}$) of the leading b -jet as well as the distance between the Z boson and the leading b -jet in the η - ϕ plane ($\Delta R^{Z,b\text{-jet}1}$). The other three figures show distributions in the inclusive 2- b -jet phase space: the transverse momentum of the leading ($p_T^{b\text{-jet}1}$) and subleading b -jet ($p_T^{b\text{-jet}2}$), and the invariant mass of the two b -jets (m_{bb}).

As observed for the fiducial rates, NLO+PS predictions fail in describing the normalization of the measured cross sections. Additionally, the shapes of some of the distributions are not reproduced particularly well. The MINNLO_{PS} predictions, on the other hand, are in agreement with data, especially for $Z+\geq 1$ - b -jet observables the central prediction is almost spot on the data points, which is remarkable considering the relatively high precision of theory predictions and measurement. In the inclusive 2- b -jet phase space the experimental errors are larger due to the lower statistics. Here, MINNLO_{PS} predicts a normalization slightly higher than the data points, but still fully covered by the uncertainties, while the differential shapes are reproduced particularly well.

An exception to the previous statements about MINNLO_{PS} is the difference observed at high $\Delta R^{Z,b\text{-jet}1}$ with the CMS data, which originates from large values of the rapidity separation between the Z boson and the leading b -jet ($\Delta y^{Z,b\text{-jet}1}$), where similar differences appear. Although less pronounced than in the 4FS, such trend is also present the 5FS predictions at large

³ We note that several NLO+PS predictions are quoted in Ref. [15]. The one quoted in Table II is the only one using the same PDF set as in our setup.

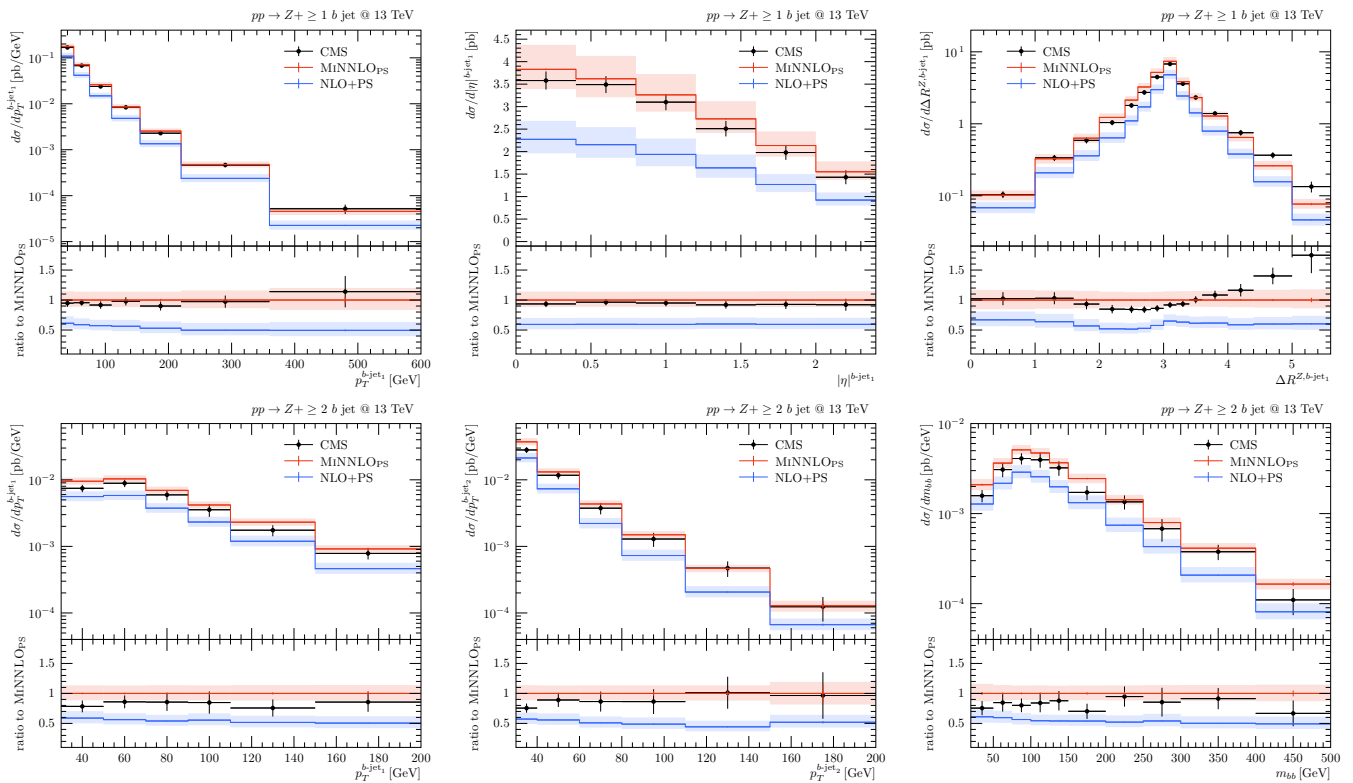


FIG. 2. Comparison of theory predictions with differential distributions measured by CMS [15].

$\Delta y^{Z,b\text{-jet}_1}$ and $\Delta R^{Z,b\text{-jet}_1}$, see Figs. 6 and 7 of Ref. [15]. That behaviour also appears in the $\Delta y^{Z,b\text{-jet}_1}$ distribution in an earlier ATLAS measurement [14]. A better understanding of this discrepancy requires additional studies and potentially all-order resummation of logarithms in m_b through a 4FS and 5FS combination at NNLO+PS, which is left for future work.

Summary.—In this letter, we presented a novel computation for the production of a Z -boson in association with bottom quarks in hadronic collisions. We have calculated NNLO QCD corrections in the 4FS, including the five-point two-loop amplitude in the small- m_b approximation. In addition, the first NNLO+PS approach for the production of a heavy-quark pair in association with colour-singlet particles has been developed, which can be readily applied to other processes, like $b\bar{b}W$ [55], $t\bar{t}W$ [77], and $t\bar{t}H$ [78] production.

Our NNLO+PS calculation solves two (related) long-standing issues for $b\bar{b}Z$ production: First, the significant tension of NLO(+PS) predictions in the 4FS with experimental data. Second, the large differences between 4FS and 5FS predictions for this process [18]. Our analysis identifies that missing higher-order corrections in the 4FS cause these discrepancies and that the

perturbative accuracy of previous calculations has been insufficient. Including NNLO QCD corrections brings the 4FS predictions in agreement with the experimental data and with the 5FS results. The calculation presented in this letter also builds the basis for a more accurate determination of the bottom-quark mass effects in Drell-Yan production, relevant for M_W measurements, along the lines of the study in Ref. [79], which at the time was pursued only at NLO+PS.

Acknowledgements.—We would like to thank Luca Buonocore, Fernando Febres Cordero, Rhorry Gauld, Massimiliano Grazzini, Pier Francesco Monni, Luca Rottoli and Giulia Zanderighi, for fruitful discussions and comments on the manuscript. We are indebted to Federico Buccioni for providing OPENLOOPS amplitudes with a different number of quarks running in the loops. We are thankful to Stefan Kallweit for helping us with a fixed-order implementation, which we used for comparison. We further thank Luca Buonocore and Luca Rottoli for performing cross checks on the massification procedure with us, and we thank Chiara Savoini and Massimiliano Grazzini for bringing to our attention the issues related to the singular behaviour of the massless amplitudes for certain mappings from the massive to the massless momenta of the bottom quarks.

-
- [1] Morad Aaboud *et al.* (ATLAS), “Measurement of the W -boson mass in pp collisions at $\sqrt{s} = 7$ TeV with the ATLAS detector,” *Eur. Phys. J. C* **78**, 110 (2018), [Erratum: *Eur.Phys.J.C* 78, 898 (2018)], [arXiv:1701.07240 \[hep-ex\]](#).
- [2] Roel Aaij *et al.* (LHCb), “Measurement of the W boson mass,” *JHEP* **01**, 036 (2022), [arXiv:2109.01113 \[hep-ex\]](#).
- [3] T. Aaltonen *et al.* (CDF), “High-precision measurement of the W boson mass with the CDF II detector,” *Science* **376**, 170–176 (2022).
- [4] Georges Aad *et al.* (ATLAS), “Measurements of WH and ZH production in the $H \rightarrow b\bar{b}$ decay channel in pp collisions at 13 TeV with the ATLAS detector,” *Eur. Phys. J. C* **81**, 178 (2021), [arXiv:2007.02873 \[hep-ex\]](#).
- [5] Armen Tumasyan *et al.* (CMS), “Measurement of simplified template cross sections of the Higgs boson produced in association with W or Z bosons in the $H \rightarrow b\bar{b}$ decay channel in proton-proton collisions at $\sqrt{s} = 13$ TeV,” (2023), [arXiv:2312.07562 \[hep-ex\]](#).
- [6] Aram Hayrapetyan *et al.* (CMS), “Search for a high-mass dimuon resonance produced in association with b quark jets at $\sqrt{s} = 13$ TeV,” *JHEP* **10**, 043 (2023), [arXiv:2307.08708 \[hep-ex\]](#).
- [7] T. Aaltonen *et al.* (CDF), “Measurement of Cross Sections for b Jet Production in Events with a Z Boson in p^- anti- p Collisions at $\sqrt{s} = 1.96$ -TeV,” *Phys. Rev. D* **79**, 052008 (2009), [arXiv:0812.4458 \[hep-ex\]](#).
- [8] Victor Mukhamedovich Abazov *et al.* (D0), “A Measurement of the Ratio of Inclusive Cross Sections $\sigma(p\bar{p} \rightarrow Z + b\text{jet})/\sigma(p\bar{p} \rightarrow Z + \text{jet})$ at $\sqrt{s} = 1.96$ TeV,” *Phys. Rev. D* **83**, 031105 (2011), [arXiv:1010.6203 \[hep-ex\]](#).
- [9] Victor Mukhamedovich Abazov *et al.* (D0), “Measurement of the Ratio of Differential Cross Sections $\sigma(p\bar{p} \rightarrow Z + b\text{jet})/\sigma(p\bar{p} \rightarrow Z + \text{jet})$ in $p\bar{p}$ Collisions at $\sqrt{s} = 1.96$ TeV,” *Phys. Rev. D* **87**, 092010 (2013), [arXiv:1301.2233 \[hep-ex\]](#).
- [10] Serguei Chatrchyan *et al.* (CMS), “Measurement of the production cross sections for a Z boson and one or more b jets in pp collisions at $\sqrt{s} = 7$ TeV,” *JHEP* **06**, 120 (2014), [arXiv:1402.1521 \[hep-ex\]](#).
- [11] Georges Aad *et al.* (ATLAS), “Measurement of differential production cross-sections for a Z boson in association with b -jets in 7 TeV proton-proton collisions with the ATLAS detector,” *JHEP* **10**, 141 (2014), [arXiv:1407.3643 \[hep-ex\]](#).
- [12] Roel Aaij *et al.* (LHCb), “Measurement of the Z + b -jet cross-section in pp collisions at $\sqrt{s} = 7$ TeV in the forward region,” *JHEP* **01**, 064 (2015), [arXiv:1411.1264 \[hep-ex\]](#).
- [13] V. Khachatryan *et al.* (CMS), “Measurements of the associated production of a Z boson and b jets in pp collisions at $\sqrt{s} = 8$ TeV,” *Eur. Phys. J. C* **77**, 751 (2017), [arXiv:1611.06507 \[hep-ex\]](#).
- [14] Georges Aad *et al.* (ATLAS), “Measurements of the production cross-section for a Z boson in association with b -jets in proton-proton collisions at $\sqrt{s} = 13$ TeV with the ATLAS detector,” *JHEP* **07**, 044 (2020), [arXiv:2003.11960 \[hep-ex\]](#).
- [15] Armen Tumasyan *et al.* (CMS), “Measurement of the production cross section for Z + b jets in proton-proton collisions at $\sqrt{s} = 13$ TeV,” *Phys. Rev. D* **105**, 092014 (2022), [arXiv:2112.09659 \[hep-ex\]](#).
- [16] Georges Aad *et al.* (ATLAS), “Measurement of cross-sections for production of a Z boson in association with a flavor-inclusive or doubly b -tagged large-radius jet in proton-proton collisions at $\sqrt{s} = 13$ TeV with the ATLAS experiment,” *Phys. Rev. D* **108**, 012022 (2023), [arXiv:2204.12355 \[hep-ex\]](#).
- [17] Georges Aad *et al.* (ATLAS), “Measurements of the production cross-section for a Z boson in association with b - or c -jets in proton-proton collisions at $\sqrt{s} = 13$ TeV with the ATLAS detector,” (2024), [arXiv:2403.15093 \[hep-ex\]](#).
- [18] Frank Krauss, Davide Napoletano, and Steffen Schumann, “Simulating b -associated production of Z and Higgs bosons with the SHERPA event generator,” *Phys. Rev. D* **95**, 036012 (2017), [arXiv:1612.04640 \[hep-ph\]](#).
- [19] F. Febres Cordero, L. Reina, and D. Wackerroth, “NLO QCD corrections to $Zb\bar{b}$ production with massive bottom quarks at the Fermilab Tevatron,” *Phys. Rev. D* **78**, 074014 (2008), [arXiv:0806.0808 \[hep-ph\]](#).
- [20] John M. Campbell and R. Keith Ellis, “Radiative corrections to Z b anti- b production,” *Phys. Rev. D* **62**, 114012 (2000), [arXiv:hep-ph/0006304](#).
- [21] John M. Campbell, R. Keith Ellis, F. Maltoni, and S. Willenbrock, “Associated production of a Z Boson and a single heavy quark jet,” *Phys. Rev. D* **69**, 074021 (2004), [arXiv:hep-ph/0312024](#).
- [22] R. Gauld, A. Gehrmann-De Ridder, E. W. N. Glover, A. Huss, and I. Majer, “Predictions for Z -Boson Production in Association with a b -Jet at $\mathcal{O}(\alpha_s^3)$,” *Phys. Rev. Lett.* **125**, 222002 (2020), [arXiv:2005.03016 \[hep-ph\]](#).
- [23] Fernando Febres Cordero, L. Reina, and D. Wackerroth, “ W - and Z -boson production with a massive bottom-quark pair at the Large Hadron Collider,” *Phys. Rev. D* **80**, 034015 (2009), [arXiv:0906.1923 \[hep-ph\]](#).
- [24] Rikkert Frederix, Stefano Frixione, Valentin Hirschi, Fabio Maltoni, Roberto Pittau, and Paolo Torrielli, “ W and Z/γ^* boson production in association with a bottom-antibottom pair,” *JHEP* **09**, 061 (2011), [arXiv:1106.6019 \[hep-ph\]](#).
- [25] Stefan Höche, Johannes Krause, and Frank Siegert, “Multijet Merging in a Variable Flavor Number Scheme,” *Phys. Rev. D* **100**, 014011 (2019), [arXiv:1904.09382 \[hep-ph\]](#).
- [26] Stefano Forte, Davide Napoletano, and Maria Ubiali, “ Z boson production in bottom-quark fusion: a study of b -mass effects beyond leading order,” *Eur. Phys. J. C* **78**, 932 (2018), [arXiv:1803.10248 \[hep-ph\]](#).
- [27] S. Abreu, F. Febres Cordero, H. Ita, M. Klinkert, B. Page, and V. Sotnikov, “Leading-color two-loop amplitudes for four partons and a W boson in QCD,” *Journal of High Energy Physics* **04**, 042 (2022), [arxiv:2110.07541 \[hep-ph\]](#).
- [28] Keith Hamilton, Paolo Oleari, and Giulia Zanderighi, “Merging $H/W/Z + 0$ and 1 jet at NLO with no merging scale: a path to parton shower + NNLO matching,” *JHEP* **05**, 082 (2013), [arXiv:1212.4504 \[hep-ph\]](#).
- [29] Simone Alioli, Christian W. Bauer, Calvin Berger, Frank J. Tackmann, Jonathan R. Walsh, and Saba Zuberi, “Matching Fully Differential NNLO Calculations and Parton Showers,” *JHEP* **06**, 089 (2014),

- arXiv:1311.0286 [hep-ph].
- [30] Stefan Höche, Ye Li, and Stefan Prestel, “Drell-Yan lepton pair production at NNLO QCD with parton showers,” *Phys. Rev. D* **91**, 074015 (2015), arXiv:1405.3607 [hep-ph].
- [31] Pier Francesco Monni, Paolo Nason, Emanuele Re, Marius Wiesemann, and Giulia Zanderighi, “MiNNLO_{PS}: a new method to match NNLO QCD to parton showers,” *JHEP* **05**, 143 (2020), arXiv:1908.06987 [hep-ph].
- [32] Pier Francesco Monni, Emanuele Re, and Marius Wiesemann, “MiNNLO_{PS}: optimizing $2 \rightarrow 1$ hadronic processes,” *Eur. Phys. J. C* **80**, 1075 (2020), arXiv:2006.04133 [hep-ph].
- [33] Javier Mazzitelli, Pier Francesco Monni, Paolo Nason, Emanuele Re, Marius Wiesemann, and Giulia Zanderighi, “Next-to-Next-to-Leading Order Event Generation for Top-Quark Pair Production,” *Phys. Rev. Lett.* **127**, 062001 (2021), arXiv:2012.14267 [hep-ph].
- [34] Javier Mazzitelli, Pier Francesco Monni, Paolo Nason, Emanuele Re, Marius Wiesemann, and Giulia Zanderighi, “Top-pair production at the LHC with MINNLO_{PS},” *JHEP* **04**, 079 (2022), arXiv:2112.12135 [hep-ph].
- [35] Javier Mazzitelli, Alessandro Ratti, Marius Wiesemann, and Giulia Zanderighi, “B-hadron production at the LHC from bottom-quark pair production at NNLO+PS,” *Phys. Lett. B* **843**, 137991 (2023), arXiv:2302.01645 [hep-ph].
- [36] Stefano Catani, Ignacio Fabre, Massimiliano Grazzini, and Stefan Kallweit, “ $t\bar{t}H$ production at NNLO: the flavour off-diagonal channels,” *Eur. Phys. J. C* **81**, 491 (2021), arXiv:2102.03256 [hep-ph].
- [37] Hua Xing Zhu, Chong Sheng Li, Hai Tao Li, Ding Yu Shao, and Li Lin Yang, “Transverse-momentum resummation for top-quark pairs at hadron colliders,” *Phys. Rev. Lett.* **110**, 082001 (2013), arXiv:1208.5774 [hep-ph].
- [38] Hai Tao Li, Chong Sheng Li, Ding Yu Shao, Li Lin Yang, and Hua Xing Zhu, “Top quark pair production at small transverse momentum in hadronic collisions,” *Phys. Rev. D* **88**, 074004 (2013), arXiv:1307.2464 [hep-ph].
- [39] Stefano Catani, Massimiliano Grazzini, and A. Torre, “Transverse-momentum resummation for heavy-quark hadroproduction,” *Nucl. Phys.* **B890**, 518–538 (2014), arXiv:1408.4564 [hep-ph].
- [40] Stefano Catani, Massimiliano Grazzini, and Hayk Sargsyan, “Transverse-momentum resummation for top-quark pair production at the LHC,” *JHEP* **11**, 061 (2018), arXiv:1806.01601 [hep-ph].
- [41] S. Catani, B. R. Webber, and G. Marchesini, “QCD coherent branching and semiinclusive processes at large x ,” *Nucl. Phys.* **B349**, 635–654 (1991).
- [42] Simone Alioli, Paolo Nason, Carlo Oleari, and Emanuele Re, “A general framework for implementing NLO calculations in shower Monte Carlo programs: the POWHEG BOX,” *JHEP* **06**, 043 (2010), arXiv:1002.2581 [hep-ph].
- [43] Tomáš Ježo and Paolo Nason, “On the Treatment of Resonances in Next-to-Leading Order Calculations Matched to a Parton Shower,” *JHEP* **12**, 065 (2015), arXiv:1509.09071 [hep-ph].
- [44] Fabio Cascioli, Philipp Maierhöfer, and Stefano Pozzorini, “Scattering Amplitudes with Open Loops,” *Phys. Rev. Lett.* **108**, 111601 (2012), arXiv:1111.5206 [hep-ph].
- [45] Federico Buccioni, Stefano Pozzorini, and Max Zoller, “On-the-fly reduction of open loops,” *Eur. Phys. J. C* **78**, 70 (2018), arXiv:1710.11452 [hep-ph].
- [46] Federico Buccioni, Jean-Nicolas Lang, Jonas M. Lindert, Philipp Maierhöfer, Stefano Pozzorini, Hantian Zhang, and Max F. Zoller, “OpenLoops 2,” *Eur. Phys. J. C* **79**, 866 (2019), arXiv:1907.13071 [hep-ph].
- [47] Stefano Catani and Massimiliano Grazzini, “QCD transverse-momentum resummation in gluon fusion processes,” *Nucl. Phys.* **B845**, 297–323 (2011), arXiv:1011.3918 [hep-ph].
- [48] Hayk Sargsyan, “Heavy-Quark Pair Production at Hadron Collider: Transverse-Momentum Resummation, NNLO Corrections and Azimuthal Asymmetries,” <https://doi.org/10.5167/uzh-142437>, Ph.D. Thesis (University of Zurich).
- [49] Thomas Becher and Matthias Neubert, “Infrared singularities of scattering amplitudes in perturbative QCD,” *Phys. Rev. Lett.* **102**, 162001 (2009), arxiv:0901.0722 [hep-ph].
- [50] Thomas Becher and Matthias Neubert, “On the Structure of Infrared Singularities of Gauge-Theory Amplitudes,” *JHEP* **06**, 081 (2009).
- [51] Stefano Catani, Simone Devoto, Massimiliano Grazzini, and Javier Mazzitelli, “Soft-parton contributions to heavy-quark production at low transverse momentum,” *JHEP* **04**, 144 (2023), arXiv:2301.11786 [hep-ph].
- [52] S. Devoto and J. Mazzitelli, in preparation.
- [53] A Mitov and S Moch, “The Singular behavior of massive QCD amplitudes,” *JHEP* **05**, 001 (2007), arxiv:hep-ph/0612149.
- [54] Guoxing Wang, Tianya Xia, Li Lin Yang, and Xiaoping Ye, “On the high-energy behavior of massive QCD amplitudes,” arXiv [hep-ph] (2023), arxiv:2312.12242 [hep-ph].
- [55] Luca Buonocore, Simone Devoto, Stefan Kallweit, Javier Mazzitelli, Luca Rottoli, and Chiara Savoini, “Associated production of a W boson and massive bottom quarks at next-to-next-to-leading order in QCD,” *Phys. Rev. D* **107**, 074032 (2023), arXiv:2212.04954 [hep-ph].
- [56] Duane A. Dicus and Scott S. D. Willenbrock, “Radiative Corrections to the Ratio of Z and W Boson Production,” *Phys. Rev. D* **34**, 148 (1986).
- [57] Lance J Dixon and Adrian Signer, “Complete O (α_s^{*3}) results for $e^+ e^- \rightarrow (\gamma, Z) \rightarrow$ four jets,” *Phys. Rev. D* **56**, 4031–4038 (1997), arxiv:hep-ph/9706285.
- [58] Simon Badger, Michal Czakon, Heribertus Bayu Hartanto, Ryan Moodie, Tiziano Peraro, Rene Poncelet, and Simone Zoia, “Isolated photon production in association with a jet pair through next-to-next-to-leading order in QCD,” arXiv [hep-ph] **10**, 071 (2023), arxiv:2304.06682 [hep-ph].
- [59] Samuel Abreu, Giuseppe De Laurentis, Harald Ita, Maximilian Klinkert, Ben Page, and Vasily Sotnikov, “Two-loop QCD corrections for three-photon production at hadron colliders,” *SciPost Physics* **15**, 157 (2023), arxiv:2305.17056 [hep-ph].
- [60] D. Chicherin and V. Sotnikov, “Pentagon functions for scattering of five massless particles,” *Journal of High Energy Physics* **20**, 167 (2020), arxiv:2009.07803 [hep-ph].
- [61] Dmitry Chicherin, Vasily Sotnikov, and Simone Zoia, “Pentagon functions for one-mass planar scattering amplitudes,” *Journal of High Energy Physics* **01**, 096 (2022), arxiv:2110.10111 [hep-ph].
- [62] Samuel Abreu, Dmitry Chicherin, Harald Ita, Ben Page,

- Vasily Sotnikov, Wladimir Tschernow, and Simone Zoia, “All Two-Loop Feynman Integrals for Five-Point One-Mass Scattering,” (2023), arXiv:2306.15431 [hep-ph].
- [63] Richard D. Ball *et al.* (NNPDF), “Parton distributions from high-precision collider data,” *Eur. Phys. J. C* **77**, 663 (2017), arXiv:1706.00428 [hep-ph].
- [64] Ansgar Denner, S. Dittmaier, M. Roth, and D. Wackerroth, “Predictions for all processes $e^+e^- \rightarrow 4$ fermions + gamma,” *Nucl. Phys. B* **560**, 33–65 (1999), arXiv:hep-ph/9904472.
- [65] Ansgar Denner, S. Dittmaier, M. Roth, and L. H. Wieders, “Electroweak corrections to charged-current $e^+e^- \rightarrow 4$ fermion processes: Technical details and further results,” *Nucl. Phys. B* **724**, 247–294 (2005), [Erratum: *Nucl. Phys. B* 854,504(2012)], arXiv:hep-ph/0505042 [hep-ph].
- [66] P. A. Zyla *et al.* (Particle Data Group), “Review of Particle Physics,” *PTEP* **2020**, 083C01 (2020).
- [67] Torbjörn Sjöstrand, Stefan Ask, Jesper R. Christiansen, Richard Corke, Nishita Desai, Philip Ilten, Stephen Mrenna, Stefan Prestel, Christine O. Rasmussen, and Peter Z. Skands, “An Introduction to PYTHIA 8.2,” *Comput. Phys. Commun.* **191**, 159–177 (2015), arXiv:1410.3012 [hep-ph].
- [68] Peter Skands, Stefano Carrazza, and Juan Rojo, “Tuning PYTHIA 8.1: the Monash 2013 Tune,” *Eur. Phys. J. C* **74**, 3024 (2014), arXiv:1404.5630 [hep-ph].
- [69] T. Kinoshita, “Mass singularities of Feynman amplitudes,” *J. Math. Phys.* **3**, 650–677 (1962).
- [70] T. D. Lee and M. Nauenberg, “Degenerate Systems and Mass Singularities,” *Phys. Rev.* **133**, B1549–B1562 (1964).
- [71] Andrea Banfi, Gavin P. Salam, and Giulia Zanderighi, “Infrared safe definition of jet flavor,” *Eur. Phys. J. C* **47**, 113–124 (2006), arXiv:hep-ph/0601139.
- [72] Simone Caletti, Andrew J. Larkoski, Simone Marzani, and Daniel Reichelt, “Practical jet flavour through NNLO,” *Eur. Phys. J. C* **82**, 632 (2022), arXiv:2205.01109 [hep-ph].
- [73] Michal Czakon, Alexander Mitov, and Rene Poncelet, “Infrared-safe flavoured anti- k_T jets,” *JHEP* **04**, 138 (2023), arXiv:2205.11879 [hep-ph].
- [74] Rhorry Gauld, Alexander Huss, and Giovanni Stagnitto, “Flavor Identification of Reconstructed Hadronic Jets,” *Phys. Rev. Lett.* **130**, 161901 (2023), arXiv:2208.11138 [hep-ph].
- [75] Fabrizio Caola, Radoslaw Grabarczyk, Maxwell L. Hutt, Gavin P. Salam, Ludovic Scyboz, and Jesse Thaler, “Flavored jets with exact anti- k_T kinematics and tests of infrared and collinear safety,” *Phys. Rev. D* **108**, 094010 (2023), arXiv:2306.07314 [hep-ph].
- [76] J. Alwall, R. Frederix, S. Frixione, V. Hirschi, F. Maltoni, O. Mattelaer, H. S. Shao, T. Stelzer, P. Torrielli, and M. Zaro, “The automated computation of tree-level and next-to-leading order differential cross sections, and their matching to parton shower simulations,” *JHEP* **07**, 079 (2014), arXiv:1405.0301 [hep-ph].
- [77] Luca Buonocore, Simone Devoto, Massimiliano Grazzini, Stefan Kallweit, Javier Mazzitelli, Luca Rottoli, and Chiara Savoini, “Precise Predictions for the Associated Production of a W Boson with a Top-Antitop Quark Pair at the LHC,” *Phys. Rev. Lett.* **131**, 231901 (2023), arXiv:2306.16311 [hep-ph].
- [78] Stefano Catani, Simone Devoto, Massimiliano Grazzini, Stefan Kallweit, Javier Mazzitelli, and Chiara Savoini, “Higgs Boson Production in Association with a Top-Antitop Quark Pair in Next-to-Next-to-Leading Order QCD,” *Phys. Rev. Lett.* **130**, 111902 (2023), arXiv:2210.07846 [hep-ph].
- [79] Emanuele Bagnaschi, Fabio Maltoni, Alessandro Vicini, and Marco Zaro, “Lepton-pair production in association with a $b\bar{b}$ pair and the determination of the W boson mass,” *JHEP* **07**, 101 (2018), arXiv:1803.04336 [hep-ph].
- [80] Werner Bernreuther and Werner Wetzel, “Decoupling of Heavy Quarks in the Minimal Subtraction Scheme,” *Nucl. Phys. B* **197**, 228–236 (1982), [Erratum: *Nucl. Phys. B* 513, 758–758 (1998)].
- [81] Andrea Ferroglia, Matthias Neubert, Ben D Pecjak, and Li Lin Yang, “Two-loop divergences of massive scattering amplitudes in non-abelian gauge theories,” *JHEP* **11**, 062 (2009).
- [82] Stefano Catani, “The Singular behavior of QCD amplitudes at two loop order,” *Phys. Lett. B* **427**, 161–171 (1998), arXiv:hep-ph/9802439.
- [83] Giuseppe De Laurentis, Harald Ita, and Vasily Sotnikov, “Double-Virtual NNLO QCD Corrections for Five-Parton Scattering: The Quark Channels,” (2023), arXiv:2311.18752 [hep-ph].
- [84] Andre van Hameren, Jens Vollinga, and Stefan Weinzierl, “Automated computation of one-loop integrals in massless theories,” *Eur. Phys. J. C* **41**, 361–375 (2005), arXiv:hep-ph/0502165.

SUPPLEMENTAL MATERIAL

Appendix A: Finite massification

In this appendix we provide additional details on the small bottom mass approximation (exploiting a massification procedure) that we use to compute the two-loop amplitude for $b\bar{b}Z$ production. The massification procedure allows us to approximate a massive amplitude from the massless one, while dropping power corrections in the bottom mass m_b , but reproducing correctly all logarithmic terms in m_b .

We aim to calculate the finite remainder $|\mathcal{R}\rangle = \mathbf{Z}^{-1} |\mathcal{M}\rangle$ defined in Eq. (4) (we leave the channel labels implicit for clarity of the formulae) in the small bottom mass approximation. Using the factorization formula from Refs. [53, 54], we obtain

$$|\mathcal{R}_{m_b \ll \mu_h}\rangle = \mathbf{Z}_{m_b \ll \mu_h}^{-1} \mathcal{F} \mathbf{S} \mathbf{Z}_0 |\mathcal{R}_0\rangle \Big|_{n_f = n_l + n_h}, \quad \text{with} \quad |\mathcal{R}\rangle = |\mathcal{R}_{m_b \ll \mu_h}\rangle + \mathcal{O}\left(\frac{m_b}{\mu_h}\right), \quad (\text{A1})$$

where μ_h is the characteristic hard scale of the process, $|\mathcal{R}_0\rangle = \mathbf{Z}_0^{-1} |\mathcal{M}_0\rangle$ is the massless finite remainder defined through the *massless* IR renormalization operator \mathbf{Z}_0 [49, 50], and $\mathbf{Z}_{m_b \ll \mu_h}$ is the small mass expansion of \mathbf{Z} . The channel-dependent operators \mathcal{F} are defined as

$$\mathcal{F}_{q\bar{q}} = \mathcal{Z}_{[Q]}\mathcal{Z}_{[q]}, \quad \mathcal{F}_{gg} = \mathcal{Z}_{[g]}\mathcal{Z}_{[g]}, \quad (\text{A2})$$

with the functions $\mathcal{Z}_{[i]}$ given in Refs. [53, 54], and \mathbf{S} is the soft function introduced in Ref. [54] that is required to approximate contributions from heavy quark loops. Here \mathbf{Z}_0 and $|\mathcal{R}_0\rangle$ depend on the total number of flavors $n_f = n_l + n_h$, which is determined by the number of $n_l = 4$ light flavours in the 4FS and $n_h = 1$ heavy flavours corresponding to the bottom quark. Since the top quark practically decouples due to its large mass, its loop corrections are expected to be negligible. Therefore, we discard contributions from top loops here.

We introduce functions $\bar{\mathcal{F}}$ and $\bar{\mathbf{S}}$ free from ϵ poles, such that $\bar{\mathcal{F}}\bar{\mathbf{S}} = \mathbf{Z}_{m_b \ll \mu_h}^{-1} \mathcal{F}\mathbf{S}\mathbf{Z}_0$. Here, $\bar{\mathcal{F}}$ is diagonal in colour space, while $\bar{\mathbf{S}}$ is a matrix in colour space. We start by writing their perturbative expansions in the strong coupling constant $\alpha_s^{n_f}$, which includes the heavy flavours in its running,

$$\bar{\mathcal{F}} = 1 + \left(\frac{\alpha_s^{n_f}}{2\pi}\right) \bar{\mathcal{F}}^{(1)} + \left(\frac{\alpha_s^{n_f}}{2\pi}\right)^2 \bar{\mathcal{F}}^{(2)} + \mathcal{O}(\alpha_s^3), \quad (\text{A3})$$

$$\bar{\mathbf{S}} = 1 + \left(\frac{\alpha_s^{n_f}}{2\pi}\right)^2 \mathbf{C}_d \mathcal{S}^{(2)} + \mathcal{O}(\alpha_s^3), \quad \mathbf{C}_d = \sum_{(i,j)} -\frac{\mathbf{T}_i \cdot \mathbf{T}_j}{2} \log\left(\frac{-s_{ij}}{\mu_R^2}\right), \quad (\text{A4})$$

where \mathbf{C}_d is the standard dipole colour-space operator (see e.g. Ref. [50]), and the coefficients are

$$\bar{\mathcal{F}}^{(1)} = 2C_F \ell_b^2 + C_F \ell_b + C_F \left(2 + \frac{\pi^2}{12}\right) + n_h \bar{\mathcal{F}}_{n_h, c\bar{c}}^{(1)}, \quad \text{with} \quad \bar{\mathcal{F}}_{n_h, q\bar{q}}^{(1)} = 0, \quad \bar{\mathcal{F}}_{n_h, gg}^{(1)} = -\frac{2}{3} \ell_b, \quad (\text{A5})$$

$$\begin{aligned} \bar{\mathcal{F}}^{(2)} = & 2C_F^2 \ell_b^4 + \ell_b^3 \left(\frac{22}{9} C_A C_F + 2C_F^2 - \frac{4}{9} C_F n_l\right) + \\ & \ell_b^2 \left(C_A C_F \left(\frac{167}{18} - \frac{\pi^2}{3}\right) + C_F^2 \left(\frac{9}{2} + \frac{\pi^2}{6}\right) - \frac{13}{9} C_F n_l\right) + \\ & \ell_b \left(C_A C_F \left(\frac{1165}{108} + \frac{14}{9} \pi^2 - 15\zeta_3\right) + C_F^2 \left(\frac{11}{4} - \frac{11}{12} \pi^2 + 12\zeta_3\right) - C_F n_l \left(\frac{77}{54} + \frac{2}{9} \pi^2\right)\right) + \\ & C_F^2 \left(\frac{241}{32} - \frac{163}{1440} \pi^4 + \pi^2 \left(\frac{13}{12} - 2 \log(2)\right) - \frac{3}{2} \zeta_3\right) + C_A C_F \left(\frac{12877}{2592} - \frac{47}{720} \pi^4 + \pi^2 \left(\frac{323}{432} + \log(2)\right) + \frac{89}{36} \zeta_3\right) - \\ & C_F n_l \left(\frac{1541}{1296} + \frac{37}{216} \pi^2 + \frac{13}{18} \zeta_3\right) + n_h \bar{\mathcal{F}}_{n_h, c\bar{c}}^{(2)}, \end{aligned} \quad (\text{A6})$$

with

$$\bar{\mathcal{F}}_{n_h, q\bar{q}}^{(2)} = -\frac{20}{9} \ell_b^3 C_F + \frac{32}{9} \ell_b^2 C_F + \ell_b C_F \left(-\frac{157}{27} - \frac{7}{18} \pi^2\right) + C_F \left(\frac{1933}{324} - \frac{13}{108} \pi^2 - \frac{7}{9} \zeta_3\right), \quad (\text{A7})$$

$$\begin{aligned} \bar{\mathcal{F}}_{n_h, gg}^{(2)} = & \ell_b^3 \left(-\frac{4}{9} C_A - \frac{28}{9} C_F\right) + \ell_b^2 \left(\frac{10}{9} C_A + \frac{7}{9} C_F\right) + \ell_b \left(C_F \left(-\frac{319}{54} - \frac{5}{18} \pi^2\right) + C_A \left(-\frac{92}{27} + \frac{\pi^2}{18}\right)\right) + \\ & C_A \left(\frac{179}{108} - \frac{5}{216} \pi^2 - \frac{7}{18} \zeta_3\right) + C_F \left(\frac{2677}{1296} - \frac{41}{216} \pi^2 - \frac{\zeta_3}{18}\right) + \frac{4}{9} n_h \ell_b^2, \end{aligned} \quad (\text{A8})$$

and

$$\mathcal{S}^{(2)} = n_h \left(-\frac{2}{3} \ell_b^2 + \frac{10}{9} \ell_b - \frac{14}{27}\right), \quad (\text{A9})$$

where $\ell_b = -\log(m_b/\mu_R)$. To match the implementation of the amplitudes in a 4FS calculation, we then convert the expansion in $\alpha_s^{n_f}$ of $\bar{\mathcal{F}}$, $\bar{\mathbf{S}}$, and the squared finite remainders into an expansion in the coupling constant $\alpha_s^{n_l}$ of the effective theory with n_h decoupled quarks [80] through a finite renormalization shift

$$\alpha_s^{n_f} = \alpha_s^{n_l} \left\{ 1 + \left(\frac{\alpha_s^{n_l}}{2\pi}\right) \frac{2}{3} \ell_b n_h + \left(\frac{\alpha_s^{n_l}}{2\pi}\right)^2 \left[\frac{4}{9} \ell_b^2 n_h^2 + \ell_b n_h \left(\frac{5}{3} C_A + C_F\right) + n_h \left(-\frac{4}{9} C_A + \frac{15}{8} C_F\right) \right] \right\}. \quad (\text{A10})$$

We note that in Ref. [81] \mathbf{Z}^{-1} is defined in the effective theory with n_h decoupled quarks. To obtain the expansions in $\alpha_s^{n_f}$ in Eqs. (A3) to (A9), we expand \mathbf{Z}^{-1} in $\alpha_s^{n_f}$ by applying the inverse of the decoupling relation (A10) [81, Section 4.2].

Finally, we calculate the two-loop contribution as

$$2 \operatorname{Re} \langle \mathcal{R}^{(0)} | \mathcal{R}^{(2)} \rangle = \frac{|\mathcal{R}^{(0)}|^2}{|\mathcal{R}_0^{(0)}|^2} 2 \operatorname{Re} \langle \mathcal{R}_0^{(0)} | \mathcal{R}_{m_b \ll \mu_h}^{(2)} \rangle + \mathcal{O}\left(\frac{m_b}{\mu_h}\right), \quad (\text{A11})$$

$$2 \operatorname{Re} \langle \mathcal{R}_0^{(0)} | \mathcal{R}_{m_b \ll \mu_h}^{(2)} \rangle = 2\bar{\mathcal{F}}^{(2)} |\mathcal{R}_0^{(0)}|^2 + \bar{\mathcal{F}}^{(1)} 2 \operatorname{Re} \langle \mathcal{R}_0^{(0)} | \mathcal{R}_0^{(1)} \rangle + \mathcal{S}^{(2)} 2 \operatorname{Re} \langle \mathcal{R}_0^{(0)} | \mathcal{C}_d | \mathcal{R}_0^{(0)} \rangle + 2 \operatorname{Re} \langle \mathcal{R}_0^{(0)} | \mathcal{R}_0^{(2)} \rangle. \quad (\text{A12})$$

Here $X^{(i)}$ with $X = \{\mathcal{R}, \bar{\mathcal{F}}, \mathcal{S}\}$ are now the coefficients in the expansion in $\alpha_s^{n_f}$, derived from their expressions expanded in $\alpha_s^{n_f}$ above and the expansion of the squared finite remainders in $\alpha_s^{n_f}$ using the decoupling relation in Eq. (A10). The logarithmic contributions in m_b are fully contained within the first three terms of Eq. (A12), while the two-loop diagrams are contained in the massless finite remainder at second order $\operatorname{Re} \langle \mathcal{R}_0^{(0)} | \mathcal{R}_0^{(2)} \rangle$, which we obtain from the analytic results of Ref. [27]. Since the results of Ref. [27] are obtained in the ‘‘Catani scheme’’ [82], we perform a finite renormalization shift (see e.g. Ref. [83]) to convert them into the scheme employed here. The coefficients $\kappa_{c\bar{c},i}$ of $\log(m_b/\mu_R)$ powers in Eq. (5) are then obtained from the first three terms on the right hand side of Eq. (A12) using the results of Eqs. (A3) to (A10).

Appendix B: Momentum mappings

In our 4FS calculation, the phase-space integration is performed assuming massive bottom quarks with $m_b \neq 0$. However, the massless finite remainder \mathcal{R}_0 entering Eq. (A11) must be evaluated on on-shell phase-space points P_0 with $m_b = 0$. We therefore need an explicit mapping of massive phase-space points P , $\eta : P \rightarrow P_0$, such that $\eta(P) = P_0 + \mathcal{O}(m_b/\mu_h)$. In addition, we have to ensure that η does not cause \mathcal{R}_0 to be evaluated near its singularities. Since the quark- and gluon-initiated channels have distinct leading order momentum flows (see Figure 1), it is useful to employ dedicated mappings $\eta_{q\bar{q}}, \eta_{gg}$ for each of the channels.

Let us first define our notation of the momenta by introducing the process as

$$p(p_1) p(p_2) \rightarrow b(p_b) \bar{b}(p_{\bar{b}}) \ell^+(p_{\ell^+}) \ell^-(p_{\ell^-}). \quad (\text{B1})$$

For $\eta_{q\bar{q}}$ we perform the simultaneous light-cone decomposition [84] of the massive bottom and anti-bottom momenta p_b and $p_{\bar{b}}$, respectively, and determine the massless momenta \hat{p}_b and $\hat{p}_{\bar{b}}$ as

$$\begin{aligned} \hat{p}_b &= \alpha^+ p_b - \alpha^- p_{\bar{b}}, & \alpha^\pm &= \frac{1}{2} \left(1 \pm \left(1 - 4 \frac{m_b^2}{m_{b\bar{b}}} \right)^{-\frac{1}{2}} \right), \\ \hat{p}_{\bar{b}} &= \alpha^+ p_{\bar{b}} - \alpha^- p_b, \end{aligned} \quad (\text{B2})$$

which preserves the total momentum $\hat{p}_{b\bar{b}} \equiv p_{b\bar{b}}$ of the $b\bar{b}$ system and prevents a collinear $g \rightarrow b\bar{b}$ splitting in the quark channel. The mapping $\eta_{q\bar{q}}$ is minimal in the sense that only the bottom-quark momenta are modified.

An undesirable side effect of the mapping $\eta_{q\bar{q}}$ (when applied in the gluon channel) is that \hat{p}_b or $\hat{p}_{\bar{b}}$ can become collinear to the initial state momenta p_1 or p_2 when the $b\bar{b}$ pair is produced at the threshold. In the gluon channel this introduces a collinear singularity, and we therefore construct η_{gg} such that it avoids these configurations. First, we set the massless momenta to

$$\hat{p}_x = p_x + \left(\sqrt{1 - \frac{m_b^2 n_x^2}{(p_x \cdot n_x)^2}} - 1 \right) \frac{(p_x \cdot n_x)}{n_x^2} n_x \quad \text{with } x \in \{b, \bar{b}\}, \quad (\text{B3})$$

$$n_x = p_x - p_1 \frac{(p_2 \cdot p_x)}{(p_1 \cdot p_2)} - p_2 \frac{(p_1 \cdot p_x)}{(p_1 \cdot p_2)}, \quad (\text{B4})$$

where n_x are transverse to both p_1 and p_2 . Then to restore momentum conservation we consider two options: Either we redistribute $\Delta p_{b\bar{b}} = p_b + p_{\bar{b}} - \hat{p}_b - \hat{p}_{\bar{b}}$ into \hat{p}_1 and \hat{p}_2 , such that $\hat{p}_{12} = \hat{p}_1 + \hat{p}_2 = p_1 + p_2 - \Delta p_{b\bar{b}}$, by performing a Lorentz boost on p_1 and p_2 in the direction $-\hat{p}_{12}$ followed by rescaling with $\sqrt{\hat{p}_{12}^2/p_{12}^2}$. Or, we redistribute $\Delta p_{b\bar{b}}$ into

the lepton momenta \hat{p}_{ℓ^+} and \hat{p}_{ℓ^-} instead. We have verified that in both cases η_{gg} avoids the collinear singularities in the massless amplitudes, but we choose the first option as our default choice, since it leaves the Z momentum untouched. Comparing the two choices, we estimated the uncertainty introduced by the mapping in the gluon channel to be at the sub-percent level and roughly of the order of the numerical error of our calculation.

Appendix C: Fiducial phase-space definition

In this Appendix we specify the set of fiducial cuts defined in the CMS analysis of Ref. [15] and used in this letter for the comparison to data. The final state under consideration contains a Z boson, decaying either to electrons or muons, and at least one (or two) b -jets.

The Z boson candidate is reconstructed from two same-flavour leptons with opposite charge, with their invariant mass $m_{\ell^+\ell^-}$ in the window $71 \text{ GeV} \leq m_{\ell^+\ell^-} \leq 111 \text{ GeV}$. The leptons are required to satisfy the constraint on their transverse momentum of $p_T^\ell > 25 \text{ GeV}$, and a requirement on their pseudo-rapidity of $|\eta^\ell| < 2.4$. Events with more than two leptons satisfying these cuts are vetoed. In addition, the leading lepton must satisfy the constraint $p_T^{\ell_1} > 35 \text{ GeV}$. The leptons are “dressed” by adding the momenta of all photons within a radius of $\Delta R^{\gamma,\ell} \leq 0.1$.

Jets are defined by clustering all light partons plus the bottom quark using the anti- k_T algorithm with a radius of $R = 0.4$. They are classified as b -jets if they contain at least one bottom-flavoured hadron and if they fulfill the transverse-momentum and pseudo-rapidity thresholds of $p_T^{b\text{-jet}} > 30 \text{ GeV}$ and $|\eta^{b\text{-jet}}| < 2.4$, respectively. In the $Z+\geq 1$ b -jet and $Z+\geq 2$ b -jets fiducial regions a reconstructed Z boson and at least one or two b -jets are required, respectively. The overlap between the leptons (from the Z boson decay) and the b -jets is removed by requiring a minimum distance of $\Delta R^{\ell,b\text{-jet}} > 0.4$ between them.